DECONVOLUTION OF CYCLO-STATIONARY PROCESSES USING HIGHER-ORDER CROSS-FREQUENCY CORRELATION

Arvid Trapp, Peter Wolfsteiner

Munich University of Applied Sciences,
Dachauer Strasse 98b, 80335 Munich, Germany

ABSTRACT

Cyclo-stationary processes induce cross-frequency correlation (CFC) into the raw spectrum of sensor signals. These stem from carrier-sideband combinations whose generating mechanism is the circular convolution of modulator and carrier. This paper proposes a deconvolution of cyclo-stationary processes in full spectral resolution to meaningfully investigate these CFC. Therefore relative phase dependencies are evaluated using fourth-order spectral analysis, which relates this deconvolution closely to trispectral analysis but also to the modulated signal bispectrum. This paper defines three spectra for analyzing cyclo-stationary processes: *(i)* a modulating spectrum with inherent elimination of stationary signal components, *(ii)* a modulating-raw frequency spectrum for designing optimal filter bands for envelope analysis, and *(iii)* a modulating-carrier spectrum accompanying peaks of the modulating spectrum with its fully-resolved carrier-frequency signature. These features are demonstrated using a real-world signal from condition monitoring.

Index Terms— amplitude modulation, cross-frequency correlation, trispectrum, condition monitoring, modulated signal bispectrum, relative phase

1. INTRODUCTION

Vibration-based condition monitoring is a widely used technique for identifying faulty components in machinery, with acceleration sensors being the preferred choice for recording its structure-borne vibration. Among the major challenges is that these signals are often composed of multiple components that superimpose at the sensor. Therefore, a central goal of vibration-based monitoring is to extract the signal components that indicate faulty components as clearly as possible from other signal components in the recordings. For critical machine elements such as rolling-element bearings and gears, band-limited envelope analysis is the most commonly used method. Envelope analysis distinguishes vibration of damaged components by its cyclo-stationary nature, characterized by a cyclic modulating function. For damaged rolling bearings or gears, these deterministic components of the envelope arise from the regular traversal of the damaged zone by load paths. The presence of these signal components not only indicates a damage but also allows for the identification of the specific component. Commonly, damaged components leave further traces in the form of their unique resonance characteristic, which provides the carrier of the cyclic modulation. This results from broadband local excitation of the damaged components. For local defects these tend to be impulsive, while for propagated damaged surfaces the excitation becomes broadband noisy. Summarized using common terminology, a damaged component typically emits a raw signal (schematically in Fig. 1) that is composed of high-frequency carriers that are modulated by a low-frequency envelope of deterministic components. These cyclic components carrying the desired information are influenced by a set of factors such as the machine's speed, kinematics, and slippage. To differentiate between the different spectra involved, the frequency variable is named f for raw-, f^* for carrier-, and f' for modulating frequencies throughout this paper.

The narrow carrier frequency band(s) with its cyclo-stationary characteristic led to the use of band-limited envelope analysis. By focusing on relevant frequency bands, the extraction of damage signatures is enhanced, resulting in an envelope spectrum of improved signal-to-noise ratio (SNR). Hence, recent research activities concentrate on the algorithmic identification of relevant frequency bands, known as frequency

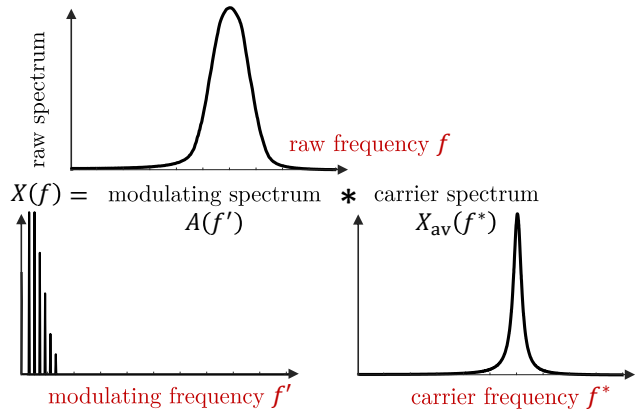

Fig. 1. Nomenclature and schematic configuration of modulated signal common in condition monitoring

band selection. Popular methods include autogram [1], infogram [2] and the use of higher-order spectral characteristics, such as spectral kurtosis analysis [3, 4], kurtogram [5] and the modulated signal bispectrum (MSB) [6]. Of these methods, the MSB differs in two significant ways, relevant for this paper. Firstly, it evaluates carrier frequencies f^* instead of raw frequencies f ('carrier frequencies and sidebands'), and secondly, it provides these in full spectral resolution, while the others operate on bands. The remainder of this paper proposes a deconvolution of the modulating mechanism by processing its cross-frequency correlation (CFC) terms. This affects all previously discussed aspects: *(i)* We introduce a modulating spectrum (MS), akin to the envelope spectrum but with less interference from additive stationary signal components and noise, due to compensation from higher-order principles; *(ii)* A modulating vs. raw frequency decomposition (MRD) resolving each peak of the MS for the raw frequencies engaged with these CFC, providing a path for defining optimal filters; *(iii)* Decomposition modulating vs. carrier frequencies (MCD) to identify a damaged component not only by its peak in the MS, but also by its unique carrier frequency signature. This signature may be shared by a set of modulating frequencies, such as higher harmonics, floating the idea of a unified damage signature; *(iv)* Normalizing these decompositions to detect weakly modulated defects.

2. FUNDAMENTALS

In order to extract meaningful information from physical measurements, such as analyzing the structure-borne vibration on a rotating machine with defective components, we face the challenge that signals $x_r(t)$ typically comprise multiple components from different sources. These can include a series of I components from regular machinery operation $x_{o,i}(t); i = 0, ..., I$; a defective component $x_{\text{dam}}(t)$, and noise $n(t)$ from inherent randomness and sensors,

$$x_r(t) = x_{o,1}(t) + ... + x_{o,I}(t) + x_{\text{dam}}(t) + n(t) \quad (1)$$

A set of challenges arise when evaluating and processing such data in the frequency domain $X(f) = \int_{-\infty}^{\infty} x(t)\, e^{-i2\pi ft}\, \mathrm{d}t$, two of which stand out in particular. Firstly, the unambiguous interpretability of the Fourier transform $X(f)$ is bound to stationarity of all components in the signal model (Eq. 1). Non-stationarity introduces spectral components — known as sidebands — representing artifacts. Secondly, source separation becomes difficult as the signal components also additively superimpose in the complex-valued frequency domain. In vibration-based condition monitoring, envelope analysis is applied to exploit that signals of a defective component $x_{\text{dam}}(t)$ can usually be distinguished by their modulated characteristic. The modulation of the carrier $x_{\text{av}}(t)$ by an envelope $a(t)$ can be expressed as $x(t) = a(t)x_{\text{av}}(t)$, where $x(t)$ could be a single-component process or any individual component of Eq. (1). The frequency-domain pendant of the modulation is the circular convolution

$$X(f) = \int_{-\infty}^{\infty} A(f')X_{\text{av}}(f^* = f - f')\, \mathrm{d}f' \quad (2)$$

When defining the expected value by $E[a(t)] = 1$, which translates to the frequency domain as $A(f' = 0) = 1$, raw $X(f)$ and carrier spectrum $X_{\text{av}}(f^*)$ only differentiate if $A(f' > 0) \neq 0$; I.e. in case $x(t)$ is non-stationary. A well-known but essential observation emerges from Eq. (2): When $x_{\text{av}}(t)$ is modulated, artifactual sidebands are induced into the raw spectrum f at frequencies different from f^* and f', whose location is determined by sum and difference frequencies $f = f^* \pm f'$. These sidebands contribute by the product of modulation- and carrier components $A(f')X_{\text{av}}(f - f')$. In other words, each raw frequency $X(f)$ consist of the corresponding carrier $X_{\text{av}}(f^* = f)$ and potentially a large sum of sideband contributions where a distant carrier frequency $f^* = f \pm f'$ is modulated by an envelope with relevant components at f' (Eq. 2). Clearly, this introduces interdependencies between frequencies of the resulting raw signal, referred to as 'cross-frequency correlation' (CFC). The challenge in deconvolving the raw spectrum of a modulated processes is that these CFC additively superimpose not only with one another (Eq. 2), but also with other signal components and noise (Eq. 1). So that in a raw spectrum, a set of signal components share a single frequency axis f, of which non-stationary components contribute with a substantial amount of superimposed sidebands, resulting from the convolution. The central challenge is to meaningfully unwind these.

3. DECONVOLUTION USING HIGHER-ORDER CROSS-FREQUENCY CORRELATION

The herein presented approach to deconvolve modulated processes is based on the relative phase dependencies of CFC terms induced by modulated signal components (Eq. 2). This section explores how these can be meaningfully processed, which interestingly leads to the definition of the fourth-order spectrum — the trispectrum.

If we approach real phenomenon from a 'microscopic' standpoint, we often find that the information carried by single Fourier coefficient limits to its amplitude $|X(f)|$ [7]. In fact, commonly to derive the information sought it requires the combination of frequencies — so that relative phase relationships come into play. Intuitively, a rationale for why frequency selection methods search for bands. To elaborate on this, consider the amplitude's companion, the phase $\varphi[X(f)]$, and a circular time shift as a demonstration for its limited explanatory value. Such a shift changes $e^{-i2\pi f\tau}$ all the individual phases differently in accordance to lag τ and individual frequency f. However, even though this rearranges a signal, its fundamental statistical characteristics remain unchanged. As such a circular shift will serve here as a simple test for

time-invariant — i.e. meaningful — descriptors. The following investigation begins by evaluating the phase relation between two raw frequencies extractable by

$$X(f_1)X^*(f_2) = |X(f_1)|\,|X(f_2)|\,e^{i(\varphi[X(f_1)]-\varphi[X(f_2)])} \quad (3)$$

To evaluate the phase difference using Eq. (3) it is necessary to take the complex conjugate of one Fourier coefficient (the choice of which to conjugate only changes the sign of the phase difference). Inserting a modulated process (Eq. 2) results in a large (equal to square of the samples) number of terms, that potentially contribute to the product of Eq. (3) ($f^* = f - f'$)

$$X(f_1)X^*(f_2) = \sum_{f_1'} A(f_1')X_{\text{av}}(f_1^*) \sum_{f_2'} A(f_2')X_{\text{av}}(f_2^*) \quad (4)$$

To reasonable limit the scope of this paper [8], it is assumed that the carrier $X_{\text{av}}(f^*)$ is subjected to distinct randomness. Specifically that its phase $\varphi[X_{\text{av}}(f^*)]$ is statistically independent. Consequently, the expected value of Eq. (4) is zero as $E[X_{\text{av}}(f_1^*)X_{\text{av}}(f_2^*)] = 0$, except for complex-conjugated pairs associated to $f_1^* + f_2^* = 0$. As such, the expected value of Eq. (4) becomes a single sum

$$E[X(f_1)X^*(f_2)] = \sum_{f^*} |X_{\text{av}}(f^*)|^2\, A(f_1 - f^*)A(f^* - f_2) \quad (5)$$

Meaningful contributions condition mutual relevant amplitudes in $X_{\text{av}}(f^*)$, $A(f_1 - f^*)$, and $A(f^* - f_2)$, where the arguments f_1 and f_2 distinctively relate the latter two by an offset $f_{12} \mathrel{\hat{=}} f_1 + f_2 = \Delta f' = (f_1 - f^*) - (f^* - f_2)$. There are three key observations to note: *(i)* Eq. (5) is exclusively determined by the phase of the modulating process $\varphi[A(f_1 - f^*)A(f^* - f_2)]$, *(ii)* the corresponding modulating frequencies are fixed to an offset $\Delta f' = f_{12}$, and *(iii)* for a low-frequency modulator $A(f')$, $|f_1|, |f_2|$ cannot deviate too much from $|f^*|$. The first observation is best illustrated when considering either $\{f_1 - f^* = 0, f^* - f_2 = 0\}$, where the resulting CFC $|X_{\text{av}}(f^*)|^2\, A(f' = f_{12})$ specifically equals the phase of the modulating function at $f' = f_{12}$. This, in principle, suggests to relate the expected value of Eq. (5) with the presence of carrier-sideband combinations $(f_1, f_2) \rightarrow (f, f \pm f_{12})$. Yet, echoing the beginning of this section, the expected value of Eq. (5) is not a time-invariant property, i.e. it is not resistant to a circular shift.

To proceed, we complete the approach by matching Eq. (5) with pairing CFC terms of inverted sign $\Delta f' = -f_{12}$, i.e. terms with opposing sidebands. Denoting the pairing frequency argument f_p, leads to the following expression:

$$X(f)X^*(f + f_{12})X(f_p)X^*(f_p - f_{12}) \quad (6)$$

Now, the expected value of Eq. (6) is substantially driven by the following real-valued terms, extending the concept of complex conjugated pairs from the carrier to the modulator:

$$\sum\nolimits_{f^*} |X_{\text{av}}(f^*)|^2\, |X_{\text{av}}(f^* + f_{1p})|^2\, |A(f')|^2\, |A(f_{12} - f')|^2 \quad (7)$$

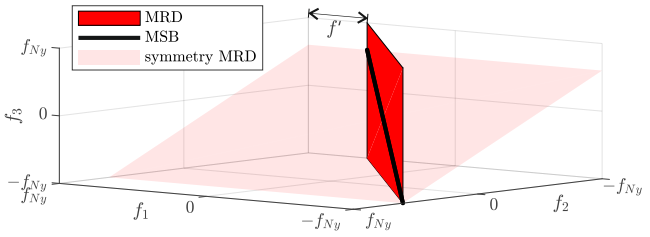

Fig. 2. Comparison of MRD and MBS in trispectral set

To piece things together, the expected value of expression (6) is zero for stationary, statistically-independent processes. However, if a modulator $A(f')$ exists composed of relevant components with frequency offset $\Delta f' = f_{12}$, its expected value gains real-valued contributions from Eq. (7) for the carriers f^* and $f^* + f_{1p}$. Under the condition of statistical stability, these contributions will stand out from those of the other signal components, which in contrast tend to an expected value of zero (e.g. signal components of Eq. 1). Moreover, these contributions indicating the presence of CFC related to f, f_p and $\Delta f' = f_{12}$ remain unaffected by any circular shift. Interestingly, the number of frequency arguments and their frequency sum in (6) corresponds to the trispectrum, providing the spectral decomposition of the kurtosis, specifically the fourth-order moment μ_4 [9]. The trispectrum $S_4(f_1, f_2, f_3) = E[X(f_1)X(f_2)X(f_3)X^*(f_1 + f_2 + f_3)]$ encompasses all products of four Fourier coefficients with a frequency sum of zero. Thus, term (6) can be interpreted as a rewritten form of decomposing the kurtosis of a modulated process into contributions of carrier-modulating CFC.

A few additional remarks are: *(i)* An offset of $\Delta f' = f_{12}$ is not only satisfied by $A(f' = 0)$ and $A(f' = f_{12})$, but also by the presence of higher harmonics in the modulator, such as $A(f' = f_{12})$ and $A(f' = 2f_{12})$. *(ii)* From a combinatorial perspective, modulating frequencies $\Delta f' = \{f_{1p}, f_{2p}\}$ can also affect Eq. (6). *(iii)* When $f_{1p} = 0$, the definition of the modulated signal bispectrum [6] is obtained. Note that this reduces the dimension by one (Fig. 2), drastically limiting statistical stability.

3.1. Deconvolution

The prior section demonstrated that fourth-order spectral analysis can statistically assess CFC resulting from circular convolution — the expected value of (6) indicates their contribution to the fourth-order moment μ_4 as cross-terms of raw frequencies f and f_p and modulator offset $\Delta f' = f_{12}$. The latter will now serve for deconvolving modulating frequencies $f' \mathrel{\hat{=}} f_{12}$. However, defining a meaningful deconvolution requires additional thoughts, to ensure statistical stability and unambiguousness. Regarding unambiguousness, we must differentiate between f and f_p as raw frequency. And in case of the former, whether f or $f + f'$ is the actual carrier

resp. sideband. Therefore, firstly

$$\begin{aligned}\mu_4^+(f', f, f_p) &= X(f)X^*(f+f')X(f_p)X^*(f_p-f') \\ \mu_4^-(f', f, f_p) &= X(f)X^*(f-f')X(f_p)X^*(f_p+f')\end{aligned} \tag{8}$$

differentiates between upper $\mu_4^+(\cdot)$ and lower $\mu_4^-(\cdot)$ carrier-sideband combinations. And secondly, to include the raw frequency controversy and — at least as important — to ensure statistical stability, we define the modulating vs. raw frequency decomposition (MRD) by

$$\mu_4(f', f) = \sum\nolimits_{f_p} \mu_4^+(f', f, f_p) + \mu_4^-(f', f, f_p) \tag{9}$$

which averages combinations of modulating f' and raw f frequency over a substantial amount of pairing frequencies f_p. Analogous to averaging for achieving statistically robust values, this simple yet effective step also eliminates f_p from (8). Further, a carrier frequency differs from a sideband in that it is centered between two complex conjugate sidebands, i.e. for a carrier $\mu_4^+(\cdot)$ and $\mu_4^-(\cdot)$ only differ in their sign. Funding on this idea, the modulating vs. carrier frequency decomposition (MCD) is defined by

$$\mu_4(f', f^*) = \sum\nolimits_{f_p} \tilde{\mu}_4^+(f', f, f_p) \cdot \tilde{\mu}_4^-(f', f, f_p) \tag{10}$$

where $\tilde{\mu}_4(\cdot)$ corresponds to Eq. (8), but its amplitude is normalized as the square root, so that MRD and MCD remain of the same unit. Finally, the modulating spectrum is defined by summation of MRD resp. MCD along the second axis f, f^*.

$$\mu_4(f') = \sum\nolimits_{f} \mu_4(f', f) \tag{11}$$

For defining a normalized MRD we specify another modification of Eq. (8) as $\mu_{|4|}(f', f)$, replacing the complex-valued Fourier coefficients with their amplitude $|X(f)|$. The normalized MRD is then defined by $\eta(f', f) = \mu_4(f', f)/\mu_{|4|}(f', f)$.

4. EXAMPLE

A few of the features of the herein proposed deconvolution are demonstrated using a dataset from the popular Case Western Reserve University (CWRU) bearing database [10]. Here, we found set X305DE interesting as not only the mechanically seeded outer race damage at $f' \approx 90.5$ Hz (fan end) is generally hard to detect, but it becomes even more difficult when applying band-limited envelope analysis on the bearings common carrier around $f \approx 3000$ Hz (benchmark [11] mostly classifies it as non detectable). Yet, the fault frequency f' appears dominant in the herein proposed non-parametric MS (Figure 3). Not only does the distinct peak hint at the damaged component, also the MRD for this frequency indicates the characteristic resonant frequencies at around $f \approx 3000$ Hz, providing a comprehensive damage indicator. The more accentuated components of the MRD at $f = [800, 1200]$ are

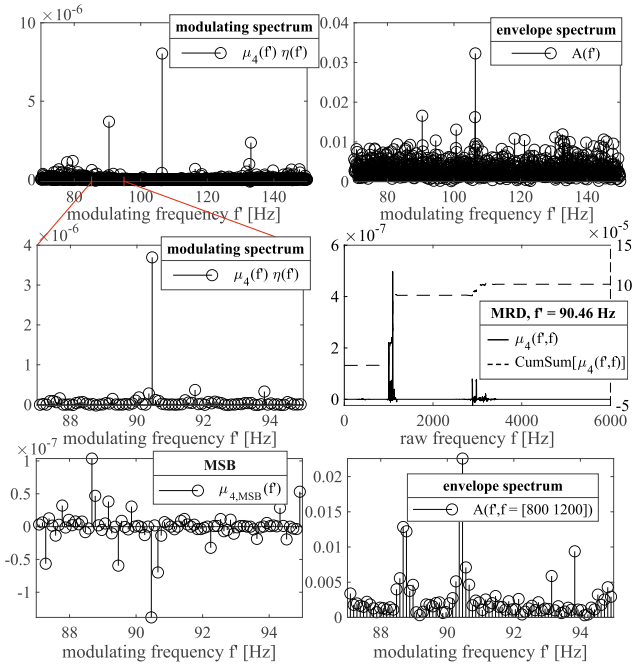

Fig. 3. Comparative analysis of dataset with seeded outer race damage $f' \approx 90.5$ Hz (CWRU database — X305DE)

then used for a band-limited envelope spectrum, giving the best result for the latter's technique. Lastly, Figure 3 includes the MSB, which apparently suffers statistically stability. In contrast, this has been achieved for the MS/MRD by summing for $f_p = [f - f' + \Delta f, f + f' - \Delta f]$ (Eq. 9).

5. CONCLUSION

Modulated processes inherent a cross-frequency structure that requires the examination of products of four Fourier coefficients for meaningful analysis. This leads to fourth-order spectral analysis, which is known as the trispectrum and involves decomposing kurtosis. In this paper, we propose a deconvolution approach for cyclo-stationary processes by associating trispectral entries with carrier-sideband combinations. The approach defines a modulating spectrum (MS) of full spectral resolution that inherently eliminates stationary signal components. It also includes decompositions of modulating vs. raw (MRD) and modulating vs. carrier frequency (MCD). These spectra eliminate the need for pre-filtering and offer additional insight into underlying signal components. While similar to the modulated signal bispectrum, the proposed deconvolution makes better use of the multidimensional trispectral set to define additional and more effective descriptors. This approach contributes to relevant subjects in vibration-based monitoring, such as improved detectability for low signal-to-noise settings, the provision of carrier frequency signatures, and optimal filter design. Overall, the proposed deconvolution provides a more effective and comprehensive analysis of cyclo-stationary processes.

6. REFERENCES

[1] A. Moshrefzadeh and A. Fasana, "The Autogram: An effective approach for selecting the optimal demodulation band in rolling element bearings diagnosis," *Mechanical Systems and Signal Processing*, vol. 105, pp. 294–318, 2018.

[2] J. Antoni, "The infogram: Entropic evidence of the signature of repetitive transients," *Mechanical Systems and Signal Processing*, vol. 74, pp. 73–94, 2016.

[3] J. Antoni, "The spectral kurtosis: a useful tool for characterising non-stationary signals," *Mechanical Systems and Signal Processing*, vol. 20, no. 2, pp. 282–307, 2006.

[4] A. Trapp and P. Wolfsteiner, "Integrated spectral kurtosis analysis," *Summit and Conference, APSIPA ASC 2021 - Proceedings*, 2021.

[5] J. Antoni, "Fast computation of the kurtogram for the detection of transient faults," *Mechanical Systems and Signal Processing*, vol. 21, no. 1, pp. 108–124, 2007.

[6] J. R. Stack, R. G. Harley, and T. G. Habetler, "An amplitude modulation detector for fault diagnosis in rolling element bearings," *IEEE Transactions on Industrial Electronics*, vol. 51, no. 5, pp. 3377–3382, 2004.

[7] B. Picinbono, "On instantaneous amplitude and phase of signals," *IEEE Transactions on Signal Processing*, vol. 45, no. 3, pp. 552–560, 1997.

[8] A. Trapp and P. Wolfsteiner, "On the generation of cross-frequency correlation in higher-order spectra arising from non-stationary processes," *Submitted for review*, 2023.

[9] C. L. Nikias and A. P. Petropulu, *Higher-order spectra analysis: A nonlinear signal processing framework*, Prentice Hall, Englewood Cliffs, NJ, 1993.

[10] Case Western Reserve University, "Bearing Data Center: Seeded Fault Test Data," https://engineering.case.edu/bearingdatacenter.

[11] W. A. Smith and R. B. Randall, "Rolling element bearing diagnostics using the Case Western Reserve University data: A benchmark study," *Mechanical Systems and Signal Processing*, vol. 64-65, pp. 100–131, 2015.